JOURNAL OF MATERIALS SCIENCE 16 (1981) 1511–1521

An activated rate theory approach to the hydrostatic extrusion of polymers

P. S. HOPE, I. M. WARD
Department of Physics, University of Leeds, Leeds, UK

An analysis of the mechanics of the hydrostatic extrusion process for polymers is presented, in which the predicted extrusion pressure is considered to be influenced by the effects of strain, strain rate and pressure on the material flow stress, as well as by the billet–die friction. The extrusion behaviour of both crystalline and amorphous polymers is discussed with reference to experimental results for linear polyethylene, polyoxymethylene and polymethylmethacrylate. Particular attention is paid to the method of incorporating the flow behaviour of the polymer into the analysis. A modified form of the Eyring equation for an activated rate process is proposed, in which the effects of strain rate and pressure on the flow stress are assumed to be separable, but related to strain by the large strain dependence of the stress activation volume. Moreover, a direct equivalence between the pressure effect and the friction between the polymer and the die is proposed for hydrostatic extrusion, following previous work on the adhesive mechanism for friction in polymers. This results in a formally identical analysis for both crystalline and amorphous polymers, in which the strain rate sensitivity, pressure sensitivity and friction coefficients all increase markedly with material strain during the process.

1. Introduction

The technique of hydrostatic extrusion was initially employed as a metal forming process by Bridgman [1] in 1952, and was first applied to the solid-phase forming of polymers by Pugh and Low [2] in 1964. Since then a good deal of experimental and analytical work has been reported on the hydrostatic extrusion of both crystalline and amorphous polymers. Although most studies have been performed on crystalline polymers, in particular linear polyethylene (LPE) [2–17], low-density polyethylene [18], polypropylene [9, 19], polyoxymethylene (POM) [9, 20], nylon-6 [9] and polytetrafluoroethylene [2], work has also been reported, to a lesser extent, on the amorphous polymers polymethylmethyacrylate (PMMA) [9, 21], polycarbonate [9, 22], polyvinyl chloride [9, 18], polysulphone [23] and polyimide [23].

Work in our laboratories was prompted by the desirability of obtaining highly oriented crystalline polymers, having similar properties to the ultra-high-modulus fibres obtained by cold drawing [24], but in sections large enough to allow the measurement of transverse properties, and to offer potential as engineering materials. The most successful results were obtained for LPE [11–16] and POM [20], for which room-temperature Young's moduli of up to 50 GPa were obtained; a variety of product sections, including square and I-section rods, circular rods and tubes, has been produced in a range of sizes up to 25 mm diameter. An analysis of the mechanics of the process has been presented previously, in which the small-scale (~ 2 mm diameter) isothermal extrusion behaviour of LPE and POM was considered to be influenced by the strain, strain rate and pressure dependence of the material flow stress, as well as by the billet–die friction coefficient [25, 26]. More recently, this analysis was applied to the hydrostatic extrusion behaviour of PMMA [21], which was under investigation with the aim

0022–2461/81/061511–11$03.10/0 © *1981 Chapman and Hall Ltd.*

TABLE I Details of polymers and hydrostatic extrusion conditions

Polymer	Manufacturer	Grade	Extrusion temperature (° C)	Die-exit diameter (mm)	Die-exit velocity (mm min^{-1})
PMMA	ICI	Perspex	90	7.0	1.0
POM	Du Pont	Delrin-500	164	1.8	0.2
LPE	BP Chemicals	Rigidex-50	100	2.5	1.0

of producing oriented amorphous materials for structural studies [27], and adequate fits to experimental data were obtained.

In the previous analysis for crystalline polymers it was necessary to postulate a multiplicative type of pressure effect in order to achieve good fits to the experimental data, while an additive pressure effect was found to give better results for amorphous polymers. In the present work an analysis is presented which is based on the same plasticity analysis of the process mechanics, but in which the effects of strain, strain rate and pressure on the material flow stress are discussed within a more consistent physical framework, namely that of an activated rate process for the plastic deformation. Both amorphous and crystalline polymers can be treated in the same fashion, so that the differences between different materials can be seen as differences in degree, rather than kind, which can hopefully then be related to differences in structure.

Moreover we explore the possibility that there is a direct equivalence between the effect of hydrostatic pressure on the yield stress and the friction between the polymer and the die; this follows recent work by Tabor and co-workers on the frictional behaviour of polymers [28, 29]. By combining this approach with the rate-theory approach it is possible to relate the very large effects on the process of strain rate, pressure and friction to a single material parameter, namely the shear activation volume.

2. Hydrostatic extrusion data

The basic process data for the analysis have been condensed from previously reported hydrostatic extrusion experiments on PMMA [21], LPE [12] and POM [20]. In each of these investigations several grades of polymer were processed under a variety of conditions, but for the purposes of our analysis the results for a single grade of each polymer are taken at a single temperature and production rate. It should be noted that the term "solid-phase extrusion" implies extrusion at a temperature below the crystalline melting point for crystalline polymers, and extrusion below the glass transition temperature for amorphous polymers.

Full details of the sample preparation, extrusion apparatus and experimental procedure may be found in the above references. It is perhaps worth noting, however, that while the production of flaw-free extrudates was relatively straightforward in the case of LPE and POM, the processing conditions for PMMA were generally far less reproducible, due to the frequent occurrence of brittle fracture of the product, and the phenomenon of "stick–slip". The extrusion behaviour of PMMA was found to be particularly sensitive to the surface condition of the billet material, the best results being obtained by a procedure in which the billets were polished, sand-blasted and then coated with a latex rubber prior to extrusion.

Information on the polymer grades and processing conditions is given in Table I. In each case the extrusion temperature is close to the optimum for the production of highly oriented products, and low die-exit diameter and die-exit velocities are chosen to ensure isothermal conditions. In all cases the die semi-angle is 15°, and the extrusion fluid is castor oil.

Fig. 1 shows plots of extrusion pressure, P, against extrusion ratio, R_N, for all three polymers under the process conditions of Table I. The nominal extrusion ratio, R_N, is defined as the billet cross-sectional area divided by the cross-sectional area of the die exit. For each polymer the extrusion pressure does not increase linearly with $\log R_N$, as would be the case for metals, but instead the pressure turns sharply upwards with extrusion ratio, until a limiting value of R_N is reached beyond which no further deformation can occur. The ability to reproduce this sharp up-turn in P against $\log R_N$ data is clearly one crucial test of any analysis of the process mechanics for polymers.

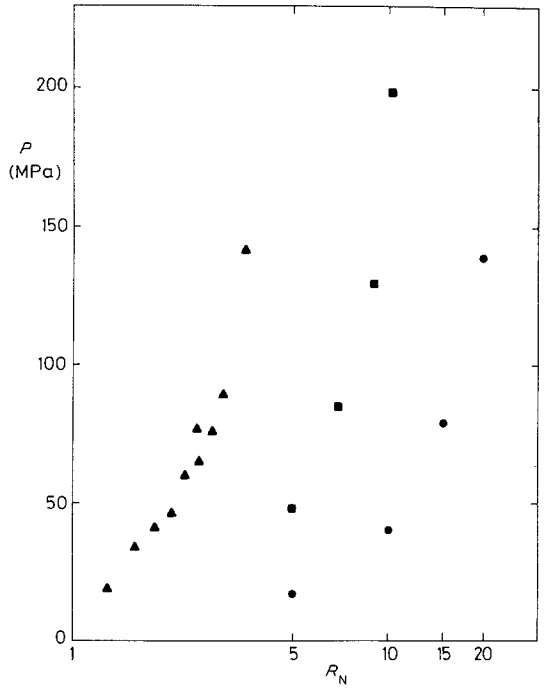

Figure 1 Experimental extrusion pressure–extrusion ratio for PMMA at 90° C (▲), POM at 164° C (■) and LPE at 100° C (●).

3. Plasticity analysis

The treatment adopted for plastic flow in a conical die is that of Hoffman and Sachs [30], which is a lower bound solution, originally developed for metals extrusion by considering the force balance on a thin, parallel-sided element in the deformation zone, giving

$$\frac{d\sigma_x}{d\epsilon} = \sigma_x - \sigma_y (1 + \mu\cot\alpha), \quad (1)$$

where μ is the billet–die friction coefficient, α is the die semi-angle, ϵ is the extensional strain, and σ_x and σ_y are the stresses parallel to and normal to the extrusion direction. For low die angles, σ_x and σ_y may be assumed to be principal stresses.

The criterion for plastic flow is that proposed by Gibson *et al.* [25, 26] based on the von Mises and Tresca yield criteria, and compatible with the Hill criterion [31] for yield of anisotropic materials, namely

$$\sigma_x - \sigma_y = \sigma_f, \quad (2)$$

where σ_f is the material flow stress. The flow stress of polymeric materials, unlike that of metals, is highly strain, strain rate, pressure and temperature dependent; hence for isothermal deformation of polymers it is necessary to modify the flow criterion to

$$\sigma_x - \sigma_y = \sigma_f(\epsilon, \dot{\epsilon}, P). \quad (3)$$

Therefore, for accurate prediction of extrusion pressures in hydrostatic extrusion, a knowledge of the true stress–strain–strain rate behaviour of the polymer is required at a range of pressures. In the absence of such data it is possible to extend true stress–strain–strain rate data obtained at ambient pressure, by assuming a linear, additive pressure effect, such that

$$\sigma_f(\epsilon, \dot{\epsilon}, P) = \sigma_f(\epsilon, \dot{\epsilon}) + \gamma' P, \quad (4)$$

where γ' is a pressure coefficient appropriate to tensile deformation. If P is taken to be the hydrostatic component of stress, the form of Equation 4 adequately describes the yield behaviour of a number of polymers [32, 33]; a physical justification for the use of a linear, additive pressure effect will be discussed in the next section. Equation 4 implies a flow criterion of the form

$$\sigma_x - \sigma_y = \sigma_f(\epsilon, \dot{\epsilon}) + \gamma' P. \quad (5)$$

While this flow criterion is suitable for isotropic materials and for materials with low degrees of anisotropy, a Coulomb yield criterion may be more appropriate for highly anisotropic materials, where one can envisage deformation occurring by slip on chains containing the *c*-axis of the polymer [34, 35]. In this case the effect of pressure on the flow stress can be regarded as entering through the effect of the normal stress σ_y, leading to a flow criterion of the form

$$\sigma_x - \sigma_y = \sigma_f(\epsilon, \dot{\epsilon}) + \gamma' \sigma_y. \quad (6)$$

In practice numerical differences in the predicted extrusion pressures resulting from the choice between the hydrostatic and normal stress formulations are small, and so the latter will be used here for ease of subsequent manipulation. Thus Equation 6 is used to eliminate σ_y from Equation 1, giving

$$\frac{d\sigma_x}{d\epsilon} = \sigma_x - \left[\frac{\sigma_x - \sigma_f(\epsilon, \dot{\epsilon})}{1 + \gamma'}\right](1 + \mu\cot\alpha). \quad (7)$$

This equation, which includes the effects of strain, strain rate and pressure on the material flow stress, as well as the effect of billet–die friction in the process, can be solved numerically, provided:

(a) the boundary conditions are specified;

(b) the strain and strain rate fields in the die are known;

(c) true stress–strain–strain rate data are available at ambient pressure (it is assumed that such data is unique at a given temperature [36]); and

(d) the pressure and friction coefficients are known.

Conditions (a) to (c) have been adequately dealt with (for the polymers under investigation) in previous publications [25, 26], and are outlined briefly in the remainder of this section. However, discussion of the effects of pressure and friction, leading to a modified form of Equation 7, will be reserved for subsequent sections.

3.1. Boundary conditions

Gibson *et al.* [25, 26] have observed that the boundary conditions for solution of Equation 7 must be modified to include the effects of redundant work (and redundant strains) at the die entrance and exit. The average redundant strain imparted at each of these boundaries is given (for spherical boundaries) by [37, 38]

$$\epsilon_{\text{red}} = \frac{1}{\sqrt{3}}\left(\frac{\alpha}{\sin^2\alpha} - \cot\alpha\right) \tag{8}$$

and the corresponding components of redundant work (per unit volume) dissipated at the entrance and exit boundaries are

$$P_1 = (\tau + \gamma\sigma_y)\,\epsilon_{\text{red}}$$

and

$$P_2 = (\tau + \gamma\sigma_y)\,\epsilon_{\text{red}}, \tag{9}$$

where τ is the shear yield stress of the isotropic material, and γ is a pressure coefficient appropriate to shear deformation. Note that $P_1 \neq P_2$, because the normal stress σ_y changes through the die. The boundary conditions therefore become

$$\text{Die entrance:} \quad \begin{cases} \sigma_x = -P + P_1, \\ \epsilon = \epsilon_{\text{red}} \end{cases}$$

$$\text{Die exit:} \quad \begin{cases} \sigma_x = -P_2, \\ \epsilon = \epsilon_{\text{red}} + \ln R_{\text{N}}. \end{cases} \tag{10}$$

In practice, for polymers the redundant work terms have a negligible effect on the final computed extrusion pressures, while the effect of modifying the strain boundary conditions is considerable, due to the large degree of strain hardening exhibited by polymers.

3.2. Strain and strain rate fields

The strain and strain rate fields in the die are simply functions of the die geometry. The strain field may be specified in terms of the instantaneous deformation ratio R as

$$\epsilon = \ln R. \tag{11}$$

Assuming a planar (plug flow) velocity profile, the strain rate field may be given by [25, 26]

$$\dot{\epsilon} = \frac{4v_{\text{f}}}{d_{\text{f}}}\left(\frac{R}{R_{\text{N}}}\right)^{3/2}\tan\alpha, \tag{12}$$

where d_{f} is the die exit diameter, and v_{f} is the velocity of the product at the die exit. For conical die extrusion (constant α) at constant velocity, Equation 12 predicts a dramatic increase in strain rate towards the die exit.

3.3. True stress–strain–strain rate data

The data presented in this section were obtained at ambient pressure. Fig. 2 contains plots of true stress against true strain, at a range of strain rates, for PMMA, POM and LPE at the relevant extrusion temperatures. The data for PMMA are taken from Hope *et al.* [21], while those for POM and LPE come from Coates and Ward [36], where full descriptions of how they were obtained can be found. The generation of such data is not straightforward, and some extrapolation was required outside the experimental range of strain rates; such regions are shown as broken curves.

While all three polymers exhibit marked strain-hardening behaviour, the degree of strain hardening is quite different for each (at the relevant temperature). Also, the sensitivity of the flow stress to strain rate increases with strain in each polymer; this is particularly evident in the case of LPE.

4. Rate theory approach to flow stress relationships

The form of the pressure-dependent flow criterion of Equation 5 may be argued from a natural extension of the Eyring equation [39] in which the plastic strain rate is expressed as

$$\dot{\epsilon} = \dot{\epsilon}_0 \exp -\left[\frac{\Delta U - \tau_{\text{f}} V + P\Omega}{kT}\right], \tag{13}$$

where $\dot{\epsilon}_0$ is a constant pre-exponential factor, ΔU is the activation energy, τ_{f} is the shear flow stress, V is the shear activation volume, Ω is the pressure activation volume, k is Boltzmann's constant and T is absolute temperature.

The shear flow stress at constant strain rate is given by

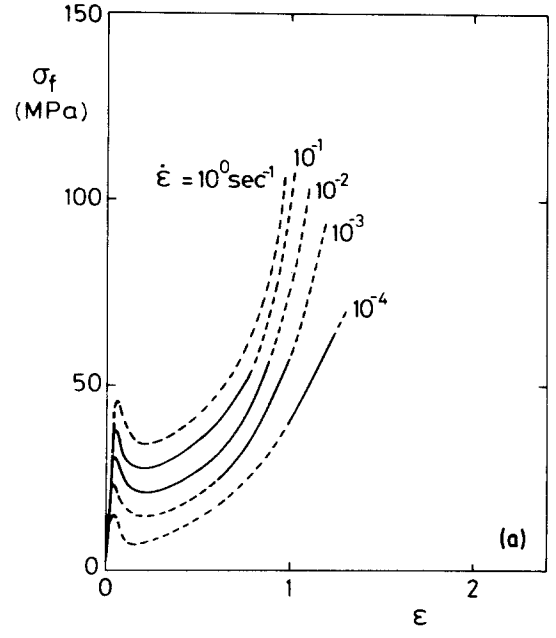

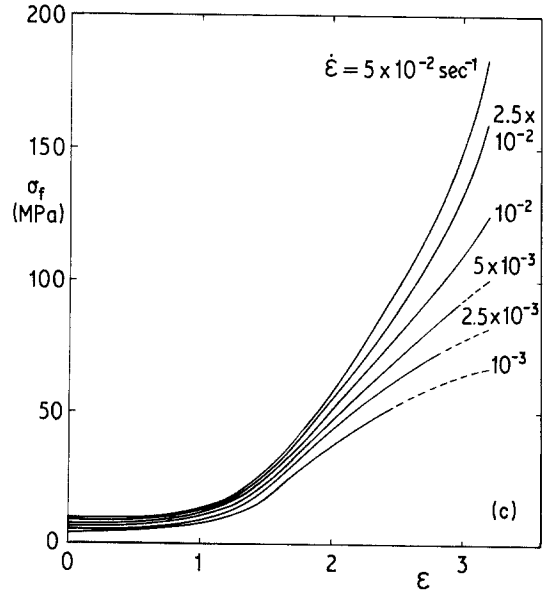

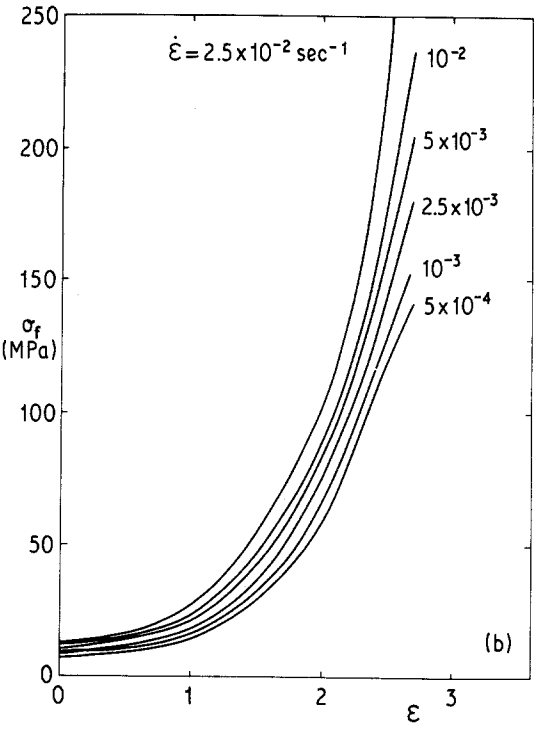

Figure 2 True stress–strain data, showing effect of strain rate. (a) PMMA at 90° C, (b) POM at 164° C, (c) LPE at 100° C.

$$\tau_f(\epsilon, \dot{\epsilon}, P) = \tau_f(\epsilon, \dot{\epsilon}) + \gamma P, \qquad (14)$$

where

$$\gamma = \left(\frac{\partial \tau_f}{\partial P}\right)_{\epsilon, T} = \frac{\Omega}{V}$$

defines the pressure dependence of the flow stress, and the parameters γ, Ω and V could in principle all be strain-dependent. Although Equation 14 is probably a more useful representation from a physical point of view than Equation 4, the two equations are formally equivalent, and we will proceed to develop Equation 4 on the basis of Equation 13 because it is a more convenient representation for considering the mechanics of the hydrostatic extrusion process, especially as we have data for σ_f as a function of ϵ and $\dot{\epsilon}$.

Equation 13 suggests that the plastic strain rate at a temperature T for any combination of tensile flow stress σ_f and hydrostatic pressure P is given by

$$\dot{\epsilon} = \dot{\epsilon}_0 \exp - \left[\frac{[\Delta U - \sigma_f(V/2 + \Omega/3) + P\Omega]}{kT}\right]. \qquad (15)$$

In a previous publication [39] $(V/2 + \Omega/3)$ has been termed the apparent activation volume for tensile flow. In this paper we will refer to $(V/2 + \Omega/3)$ as the stress activation volume, and denote it by V'. We then have

$$\sigma_f(\epsilon, \dot{\epsilon}, P) = \sigma_0(\epsilon) + k'(\epsilon) \ln \dot{\epsilon} + \gamma'(\epsilon) P \qquad (16)$$

in which

$$\sigma_0(\epsilon) = \frac{1}{V'(\epsilon)} (\Delta U - kT \ln \dot{\epsilon}_0), \qquad (17)$$

$$k'(\epsilon) = kT/V'(\epsilon) \qquad (18)$$

and

$$\gamma'(\epsilon) = \Omega(\epsilon)/V'(\epsilon). \qquad (19)$$

A number of important observations may be made from inspection of Equation 16. Firstly, the form of the equation is quite compatible with that of Equations 4 and 5, in that the effect of pressure on the flow stress enters in a linear, additive fashion. Secondly, although the effects of strain rate and pressure are separable, they are both related to strain. In the case of strain rate, the strain dependence arises as a consequence of the strain dependence of the stress activation volume (Equation 18); the strain dependence of the pressure effect, however, arises from the strain dependence of both the stress activation volume and the pressure activation volume (Equation 19).

4.1. Strain-rate sensitivity

The increase of strain-rate sensitivity with strain is seen clearly in Fig. 3, in which the flow stress is plotted against log (strain rate) for a range of strains. Returning to the theory for an activated rate process, differentation of Equation 16 yields

$$\left(\frac{\partial \sigma_f}{\partial \ln \dot{\epsilon}}\right)_{\epsilon,P} = k'(\epsilon) = \frac{kT}{V'(\epsilon)}. \qquad (20)$$

This implies that for a single, activated process, the stress–log (strain rate) relationship should be linear, with a slope inversely proportional to the stress activation volume V'. The relationships for PMMA are clearly linear over the observed range of strain rates, but imply a reduction in V' with strain. The relationships for POM and LPE, however, show a degree of non-linearity, particularly at high strains.

The apparent change in stress activation volume with strain and strain rate may be explained in terms of two or more activated processes operating in parallel, each following the Eyring formulation and representing physically separate processes [40, 41]. This suggestion is supported by recent work on yield and creep behaviour of drawn LPE carried out in our laboratories [42]. The observed curvature for POM and LPE in Fig. 3 may then be explicable in terms of the superposition of high-stress, low-activation-volume process (operating at high strain rates) onto a low-stress, high-activation-volume process (operating over the range of strain rates, but dominant at low strain rates).

In hydrostatic extrusion most of the work of deformation takes place in the region of the die exit, and it can be shown (by reference to Equation 12) that the strain rate experienced in this

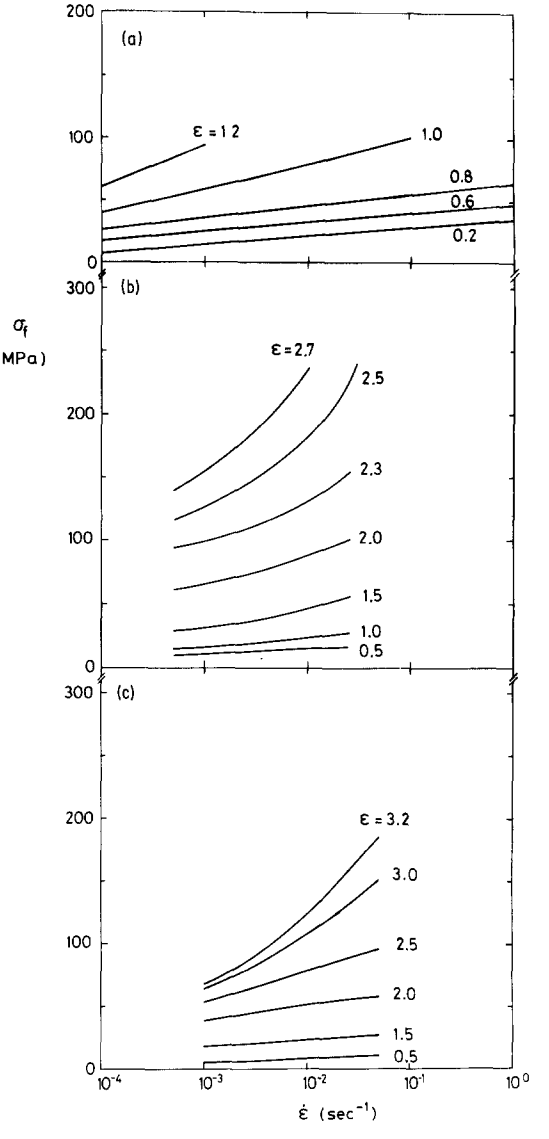

Figure 3 True stress–strain rate data, showing effect of strain rate. (a) PMMA at 90° C, (b) POM at 164° C, (c) LPE at 100° C.

region, especially for higher extrusion ratios, is such that the high-stress, low-activation-volume process dominates. Coates and Ward have proposed that an apparent stress activation volume can be obtained by measuring the slope of σ_f against ln $\dot{e}$ data at appropriately high strain rates. Operational values of V' measured in this way may then be regarded as characteristic of those experienced during the hydrostatic extrusion process. It should be noted that for POM the slope of the curves at high strain rates is not well defined for high strains, and so a range of V' values are given. In Fig. 4 the apparent stress activation volumes

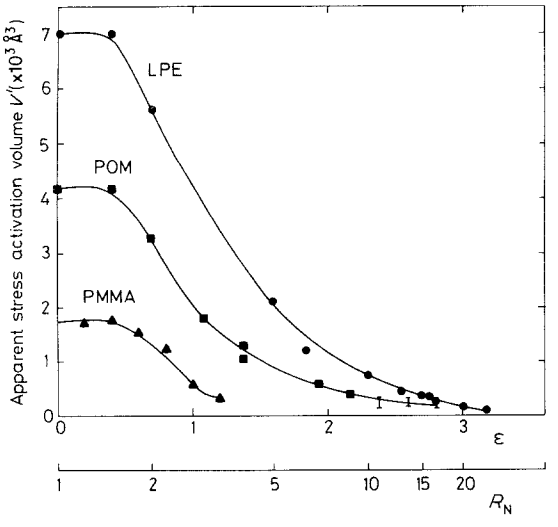

Figure 4 Apparent stress activation volume against true strain for PMMA, POM and LPE at relevant extrusion temperatures.

of all three polymers decrease markedly with strain, from an isotropic value of several thousand to a few hundred cubic angstroms at the highest strains achieved. Such large changes in V' may be related to changes in the polymer structure with strain, particularly in the crystalline polymers, where the spherulitic morphology of the isotropic material is transformed to a fibrillar structure. The fall off in V' with strain implies a marked increase in strain-rate sensitivity; it is clear from Fig. 5, in which the reciprocal of V' is plotted against strain, that the increased strain rate sensitivity is particularly marked in the case of LPE, as was noted previously.

4.2. Pressure sensitivity

While the strain-rate sensitivity is determined solely by the stress activation volume, Equation 19 suggests that a knowledge of the pressure activation volume is also required to determine the pressure sensitivity. In principle Equation 16 may be differentiated to give

$$\left(\frac{\partial \sigma_f}{\partial P}\right)_{\epsilon,\dot{\epsilon}} = \gamma'(\epsilon) = \frac{\Omega(\epsilon)}{V'(\epsilon)}. \qquad (21)$$

Evaluation of $\Omega(\epsilon)$ would therefore require true stress–strain–strain rate data at a range of pressures. Although such data is not available at the temperatures required, or over the wide range of strains required, estimates suggest that typical values of Ω for isotropic polymers lie in the region of a few hundred cubic angstroms, and do not change significantly with temperature [43, 44]. There is also evidence that the strain dependence of Ω is slight by comparison to the strain dependence of V' [45]. The stress activation volume V' is determined largely by the shear activation volume V which relates to the specific shear deformation mechanism and can be regarded as representing the volume swept out by the activated event. It is therefore not surprising that V' is much affected by permanent plastic deformation, which causes a high degree of molecular orientation. Very large activation volumes (~ 1000 Å^3) are usual for isotropic polymers and have been taken to indicate the comparatively large-scale co-operative nature of the yield process. The activation volume falls with increasing orientation due to the localization of the yield process. This is most

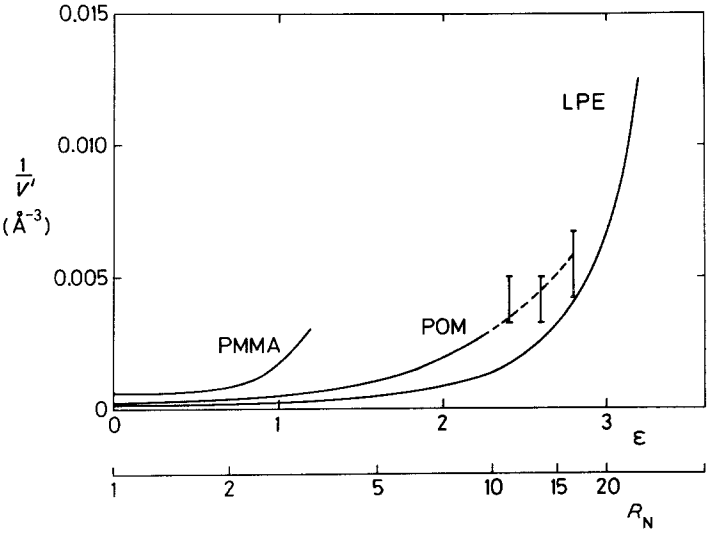

Figure 5 Inverse stress activation volume against true strain for PMMA, POM and LPE at relevant extrusion temperatures.

marked for oriented crystalline polymers, where a fibrillar texture exists and the shear activation volume (~ 100 Å^3) can be identified with a localized crystal slip process such as the movement of a Reneker defect through the crystal lattice [46].

It is reasonable to expect that the smaller pressure activation volume Ω will change much less with plastic deformation. It will relate primarily to average intermolecular distances, which, like the density, will not change greatly as the polymer is transformed from an isotropic to an oriented structure.

For the purposes of analysing the hydrostatic extrusion behaviour of polymers it is reasonable, therefore, to assume that Ω is small relative to V', and is independent of strain. This suggests that the pressure sensitivity of the polymers also follows the reciprocal relationship of Fig. 5 with strain, and that the pressure sensitivity increases rapidly at high strains, especially in the case of LPE. To accommodate this variation in the plasticity analysis it is therefore proposed that the pressure coefficient should be strain dependent, and in the absence of $\Omega(\epsilon)$ data a constant value of Ω is chosen, whence

$$\gamma'(\epsilon) = \frac{\Omega}{V'(\epsilon)}. \tag{22}$$

5. Equivalence of friction and pressure effects

A correlation between friction and pressure effects has been suggested previously [21], following the work of Briscoe and Tabor on the shear and friction properties of thin polymer films [28, 29]. In sliding tests on polymer films the shear strength τ was found to be related to the contact stress σ_p by a relationship similar in form to Equation 14, namely

$$\tau = \tau_0 + \gamma\,\sigma_p, \tag{23}$$

where τ_0 is the shear strength of the polymer film at zero contact stress, and γ is again a pressure coefficient. Consideration of the frictional force arising as a result of a shearing process within (or at the surface of) the polymer leads to an adhesive coefficient of friction given by

$$\mu = (\tau_0/\sigma_p) + \gamma. \tag{24}$$

In the case of thin polymer films, τ_0 is very much lower than the bulk value for the isotropic polymer; if we assume that this is the case during hydrostatic extrusion, and that for hydrostatic extrusion the contact stress σ_p can be replaced by the normal stress σ_y, then the first term in Equation 24 becomes small compared to the second, so that $\mu \simeq \gamma$. To make use of this relationship in our analysis it is necessary to consider the pressure coefficient relevant to tensile deformation; having regard to the hydrostatic component of stress present during tensile deformation, it may readily be shown that

$$\gamma = \frac{\gamma'}{2(1-\gamma'/3)}, \tag{25}$$

which, to a good approximation, is

$$\gamma = \frac{\gamma'}{2}. \tag{26}$$

As the pressure coefficient is strain-dependent, a strain-dependent friction coefficient is implied, such that

$$\mu(\epsilon) = \frac{\gamma'(\epsilon)}{2} = \frac{\Omega}{2V'(\epsilon)}. \tag{27}$$

This is not unreasonable physically, although no supporting experimental evidence exists independently at present. The equivalence of pressure and friction, and their strain dependence, may then be incorporated into the plasticity analysis by modification of Equation 7 to give

$$\frac{d\sigma_x}{d\epsilon} = \sigma_x - \left[\frac{\sigma_x - \sigma_f(\epsilon, \dot{\epsilon})}{1+\gamma'(\epsilon)}\right][1 + \mu(\epsilon)\cot\alpha] \tag{28}$$

in which both $\gamma'(\epsilon)$ and $\mu(\epsilon)$ are given by Equation 28. With the assumption of a constant value for Ω, the analysis may now be performed in terms of a single parameter, γ'.

6. Results and discussion

Equation 28 was solved numerically, for the appropriate boundary conditions (Equation 10), for a range of values of Ω for each polymer. The predicted variations of extrusion pressure with extrusion ratio are shown in Fig. 6. The case $\Omega = 0$ corrrsponds to conditions of zero friction and zero pressure effect; in this case the upward curvature is due entirely to the strain and strain-rate sensitivity of the flow stress, and is clearly inadequate for modelling of the experimental extrusion pressures. If, however, suitable values of Ω are chosen, then the increasing effects of friction and pressure with strain reproduce the experi-

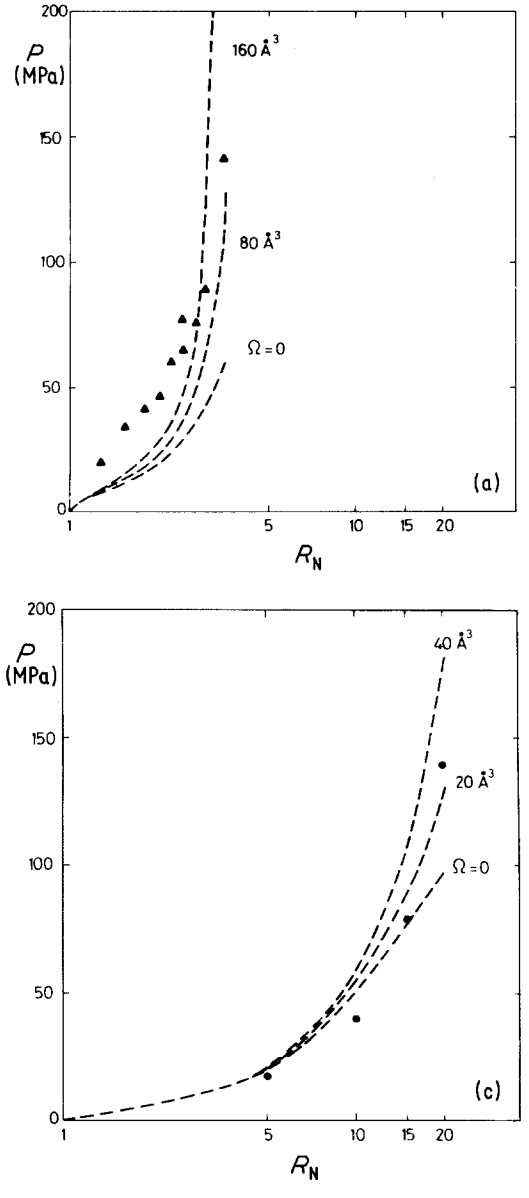

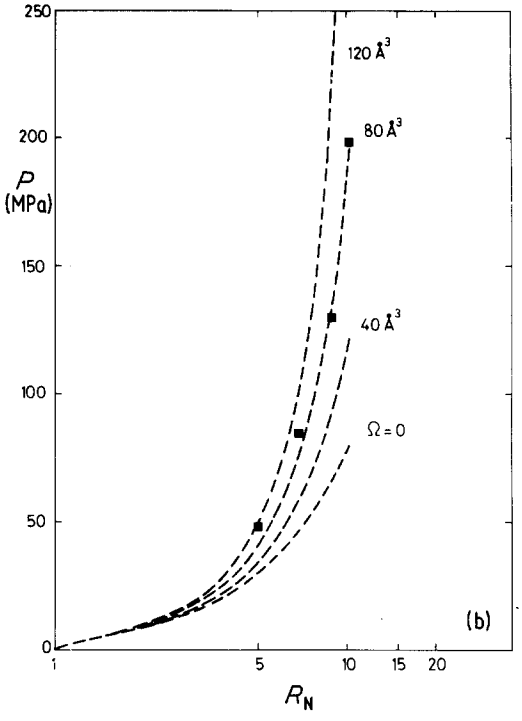

Figure 6 Comparison of experimental and analytical extrusion pressures; for full extrusion conditions see Table I. (a) PMMA at 90° C, (b) POM at 164° C, (c) LPE at 100° C.

mentally observed up-turn in pressure quite satisfactorily.

The best (least-squares) fits to the experimental extrusion data for all three polymers are shown in Fig. 7. The limiting value of extrusion ratio for each polymer, at which the up-turn in extrusion pressure inhibits further deformation, appears to correspond reasonably well to that at which the reciprocal stress activation volume turns sharply upwards in Fig. 5, confirming that the flow-stress behaviour of the polymer is the major controlling factor in hydrostatic extrusion. This is perhaps intuitively obvious from comparison of Figs 2 and 6. More specifically, it may be argued that the changes in both strain-rate sensitivity and pressure sensitivity of the polymer with strain, as characterized by the reciprocal stress activation volume, are crucial factors governing the hydrostatic extrusion behaviour of polymers. The importance of strain-rate sensitivity, particularly in a process such as conical die extrusion, where the strain rate increases dramatically towards the die exit, has been recognized previously. It is proposed here that the pressure sensitivity is equally important, and moreover is controlled by the same material parameter, namely the stress activation volume.

The values of pressure activation volume which give the best fits of Fig. 7 are shown in Table II. These values appear to be rather lower than previous estimates of Ω at low strains [43–45]; this suggests that Ω may in fact decrease slightly with strain, as the predicted values for best fits are biased towards high strain, where the pressure up-turn is steepest.

Table II also contains the range of values of friction (or pressure) coefficients predicted by the best fits to experimental data. The minimum values quoted are those at the die entrance, which for all the polymers appear to be very low, and similar to

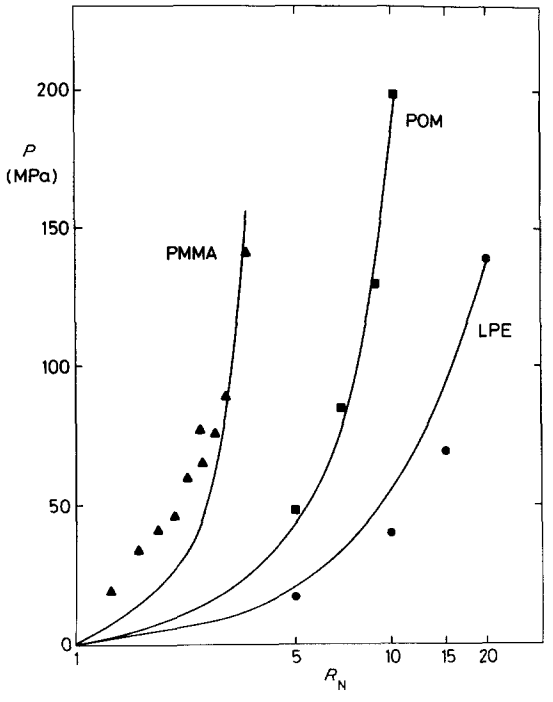

Figure 7 Best analytical fits to experimental extrusion pressure–extrusion ratio data; for full extrusion conditions see Table I.

the friction coefficients observed in metals extrusion, where hydrodynamic lubrication is known to occur. The maximum values are those at the die exit, for the largest extrusion ratio in each polymer. These values are much higher, suggesting conditions of boundary lubrication. This is consistent with the assumption of polymer-to-metal contact, inherent in the introduction of the equivalence of friction and pressure effects. While boundary lubrication is suggested at the die exit for limiting extrusion ratios, it is clear from the low values of μ that hydrodynamic lubrication may occur elsewhere. This is reasonable, as a film of fluid may well become entrained between billet and die close to the die entrance.

A third set of friction coefficients is presented in Table II at a constant extrusion ratio (R_N = 3.5). At this extrusion ratio the friction coefficient for PMMA is clearly very much higher than that of either POM or LPE. This is consistent with the occurrence of friction-controlled "stick–slip" behaviour in PMMA extrusions, a phenomenon which has not been encountered in the extrusion of POM or LPE under isothermal conditions (although thermally controlled "stick–slip" has been reported for non-isothermal extrusions [19, 12–15]). The greater importance of friction in the hydrostatic extrusion of PMMA is also consistent with the requirement for careful preparation of the billet surface prior to extrusion.

TABLE II Plasticity analysis parameters giving best fits to experimental data

Polymer	Ω (Å^3)	Friction (pressure) coefficients		
		Minimum	$R_N = 3.5$	Maximum
PMMA	100	0.029	0.187	0.187
POM	80	0.101	0.034	0.150
LPE	22	0.002	0.004	0.091

7. Conclusions

The hydrostatic extrusion behaviour of both amorphous and crystalline polymers may be modelled by a formally identical analysis, based on a knowledge of the true stress–strain–strain-rate behaviour of the polymer at ambient pressure, provided (a) the pressure dependence of the flow stress is known, and (b) the billet–die friction behaviour is known.

By the use of a rate theory approach to plastic deformation, we have assumed that the effects of strain rate and pressure on the flow stress are separable, but that both are strain-dependent. If the further reasonable assumption is made that the pressure activation volumes of polymers are relatively independent of strain, and small in comparison to their stress activation volumes, then both the strain-rate and pressure dependence are inversely proportional to the stress activation volume. In addition, it has been proposed for hydrostatic extrusion that the effects of pressure and friction are equivalent, and so for the purposes of the plasticity analysis, the friction coefficient may also be considered as inversely proportional to the stress activation volume of the polymer.

It is likely that the apparent stress activation volumes of the polymers considered here all decrease rapidly with increasing strain, as a result of the structural changes which occur on deformation. The limiting deformation ratio for each polymer may therefore be explained on the basis of the marked increase in flow stress, which accompanies the rising effects of strain rate, pressure and friction as the material passes through the deformation zone. This contrasts with tensile drawing, in which pressure and friction effects do not occur.

The friction coefficients predicted by the analysis are in line with static values, although they are generally rather lower. The friction coefficients

for PMMA at a given extrusion ratio are significantly higher than those of POM and LPE, which is consistent with the sensitivity of PMMA extrusion behaviour to the surface treatment of the starting billet.

References

1. P. W. BRIDGMAN, "Studies in Large Plastic Flow and Fracture", (McGraw-Hill, New York, 1952).
2. H. LI, D. PUGH and A. H. LOW, *J. Inst. Metals* **93** (1964–65) 201.
3. A. BUCKLEY and H. A. LONG, *Polymer Eng. Sci.* **9** (1969) 115.
4. K. NAKAYAMA and H. KANETSUNA, *Kobunshi Kagaku* **30** (1973) 713.
5. *Idem, ibid* **31** (1974) 256.
6. *Idem, ibid* **31** (1974) 321.
7. *Idem, J. Mater. Sci.* **10** (1975) 1105.
8. *Idem, ibid* **12** (1977) 1477.
9. T. NAKAYAMA and N. INOUE, *Bull. JSME* **20** (1977) 688.
10. D. M. BIGG, E. G. SMITH, M. M. EPSTEIN and R. J. FIORENTINO, *Polymer Eng. Sci.* **18** (1978) 908.
11. A. G. GIBSON, I. M. WARD, B. N. COLE and B. PARSONS, *J. Mater. Sci.* **9** (1974) 1193.
12. A. G. GIBSON and I. M. WARD, *J. Polymer Sci., Polymer Phys. Ed.* **16** (1978) 2015.
13. P. S. HOPE, A. G. GIBSON, B. PARSONS and I. M. WARD, *Polymer. Eng. Sci.* **20** (1980) 540.
14. P. S. HOPE and B. PARSONS, *Polymer Eng. Sci.* **20** (1980) 589.
15. *Idem, ibid* **20** (1980) 597.
16. P. S. HOPE, A. G. GIBSON and I. M. WARD, *J. Polymer Sci., Polymer Phys. Ed.* **18** (1980) 1243.
17. R. GUPTA and P. G. McCORMICK, *J. Mater Sci.* **15** (1980) 619.
18. J. M. ALEXANDER and P. J. H. WORMELL, *Ann. CIRP* **19** (1971) 21.
19. T. WILLIAMS, *J. Mater. Sci.* **8** (1973) 59.
20. P. D. COATES and I. M. WARD, *J. Polymer Sci., Polymer Phys. Ed.* **16** (1978) 2031.
21. P. S. HOPE, I. M. WARD and A. G. GIBSON, *J Mater. Sci.* **15** (1980) 2207.
22. P. S. HOPE and I. M. WARD, unpublished work.
23. K. D. PAE, S. K. BHATEJA and J. A. SAUER, Proceedings of the NEL/AIRAPT International conference on Hydrostatic Extrusion, NEL, Glasgow, 1973.
24. A. CIFERRI and I. M. WARD (editors), "Ultra-High Modulus Polymers", (Applied Science, London, 1979).
25. A. G. GIBSON, P. D. COATES and I. M. WARD, in "Science and Technology of Polymer Processing", edited by N. P. Suh and N. H. Sung (MIT Press, Massachussetts, 1979).
26. P. D. COATES, A. G. GIBSON and I. M. WARD, *J. Mater. Sci.* **15** (1980) 359.
27. N. KAHAR, R. A. DUCKETT and I. M. WARD, *Polymer* **19** (1978) 136.
28. B. J. BRISCOE and D. TABOR, in "Polymer Surfaces", edited by D. T. Clark and W. J. Feast (Wiley Interscience, New York, 1978) Ch. 1.
29. *Idem, J. Adhesion* **9** (1978) 145.
30. O. HOFFMAN and G. SACHS, "Introduction to the Theory of Plasticity for Engineers" (McGraw-Hill, New York, 1953).
31. R. HILL, "The Mathematical Theory of Plasticity" (Clarendon Press, Oxford, 1950).
32. D. R. MEARS, K. D. PAE and J. A. SAUER, *J. Appl. Phys.* **40** (1969) 4229.
33. S. RABINOWITZ, I. M. WARD and J. S. C. PARRY, *J. Mater. Sci.* **5** (1970) 29.
34. A. KELLER and J. G. RIDER, *ibid* **1** (1966) 389.
35. P. B. BOWDEN and J. A. JUKES, *ibid* **3** (1968) 183.
36. P. D. COATES and I. M. WARD, *ibid* **13** (1978) 1959.
37. B. AVITZUR, "Metal Forming: Processes and Analysis", (McGraw-Hill, New York, 1968).
38. H. LI, D. PUGH, "Mechanical Behaviour of Materials under Pressure", (Elsevier, Amsterdam, 1970).
39. I. M. WARD, *J. Mater. Sci.* **6** (1971) 1397.
40. C. BAUWENS-CROWET, J. C. BAUWENS and G. HOMES, *ibid* **7** (1972) 176.
41. C. BAUWENS-CROWET, *ibid* **8** (1973) 968.
42. M. A. WILDING, C. J. FRYE and I. M. WARD, *Polymer* (in press).
43. R. TRUSS, R. A. DUCKETT and I. M. WARD, *J. Mater. Sci.* (in press).
44. S. H. JOSEPH and R. A. DUCKETT, *Polymer* **19** (1978) 837.
45. L. A. DAVIS and C. A. PAMPILLO, *J. Appl. Phys.* **42** (1971) 4659.
46. D. H. RENEKER, *J. Polymer Sci.* **59** (1962) 539.

Received 16 September and accepted 13 October 1980.